NACA RM A51E01

NACA

RESEARCH MEMORANDUM

LIFT, DRAG, AND PITCHING MOMENT OF LOW-ASPECT-RATIO WINGS AT SUBSONIC AND SUPERSONIC SPEEDS - TWISTED AND CAMBERED TRIANGULAR WING OF ASPECT RATIO 2 WITH NACA 0003-63 THICKNESS DISTRIBUTION

By Charles F. Hall and John C. Heitmeyer

Ames Aeronautical Laboratory
Moffett Field, Calif.

NATIONAL ADVISORY COMMITTEE
FOR AERONAUTICS

WASHINGTON
June 12, 1951
Declassified February 26, 1958

NATIONAL ADVISORY COMMITTEE FOR AERONAUTICS

RESEARCH MEMORANDUM

LIFT, DRAG, AND PITCHING MOMENT OF LOW-ASPECT-RATIO WINGS AT SUBSONIC AND SUPERSONIC SPEEDS - TWISTED AND CAMBERED TRIANGULAR WING OF ASPECT RATIO 2 WITH NACA 0003-63 THICKNESS DISTRIBUTION

By Charles F. Hall and John C. Heitmeyer

SUMMARY

A wind-tunnel investigation has been performed at subsonic and supersonic Mach numbers to determine the aerodynamic characteristics of a wing-body combination having a triangular wing of aspect ratio 2. The mean surface of the wing was twisted and cambered to support a nearly elliptical span load distribution at a Mach number of 1.53 and a lift coefficient of 0.25. The NACA 0003-63 thickness distribution was used in combination with the theoretically determined mean lines to make up the streamwise airfoil sections. The lift, drag, and pitching moment of the model are presented for Mach numbers from 0.60 to 0.90 and from 1.30 to 1.70 at Reynolds numbers of 3.0 million and 7.5 million.

INTRODUCTION

A research program is in progress at the Ames Aeronautical Laboratory to ascertain experimentally at subsonic and supersonic Mach numbers the characteristics of wings of interest in the design of high-speed fighter airplanes. The effects of variations in plan form, twist, camber, and thickness are being investigated. This report is one of a series pertaining to this program and presents results of tests of a wing-body combination having a triangular wing of aspect ratio 2 with NACA 0003-63 thickness distribution in streamwise planes, and twisted and cambered to support a nearly elliptical spanwise loading at the design conditions. Results of other investigations in this program are presented in references 1 to 7. As in these references, the data herein are presented without analysis to expedite publication.

NOTATION

b	wing span
$\bar{c}$	mean aerodynamic chord $\left(\frac{\int_0^{b/2} c^2 dy}{\int_0^{b/2} c\, dy}\right)$
c	local wing chord projected in the wing reference plane[1]
c_r	root chord
l	length of body including portion removed to accommodate sting
$\frac{L}{D}$	lift–drag ratio
$\left(\frac{L}{D}\right)_{max}$	maximum lift–drag ratio
M	Mach number
m	β cot (angle of sweepback of leading edge of constant–load sector)
m_o	β cot Λ
n	arbitrary positive number
Δp	pressure difference between upper and lower surface, positive in sense of a lift
q	free–stream dynamic pressure
R	Reynolds number based on mean aerodynamic chord
r	radius of body
r_o	maximum body radius

[1]Wing reference plane is defined as the plane perpendicular to the plane of symmetry and containing the wing chord in the plane of symmetry.

S	total wing area projected in wing reference plane, including area enclosed by fuselage
x,y,z	Cartesian coordinates in streamwise, spanwise, and vertical directions, respectively, and with orgin located at wing apex
x'	longitudinal distance from nose of body
X	longitudinal distance from wing leading edge in wing reference plane[1]
Z	vertical distance from wing reference plane[1]
α	angle of attack of the body axis, degrees
β	$\sqrt{M^2-1}$
Λ	angle of sweepback of leading edge, degrees
ξ	value of x at the Mach cone in the $z=0$ plane
c_l	section lift coefficient $\left(\frac{\text{section lift}}{qc}\right)$
C_D	drag coefficient $\left(\frac{\text{drag}}{qS}\right)$
C_L	lift coefficient $\left(\frac{\text{lift}}{qS}\right)$
$C_{L_{des}}$	design lift coefficient
C_m	pitching-moment coefficient about the 25-percent position of the wing mean aerodynamic chord $\left(\frac{\text{pitching moment}}{qS\bar{c}}\right)$
$\frac{dC_L}{d\alpha}$	slope of the lift curve measured at zero lift, per degree
$\frac{dC_m}{dC_L}$	slope of the pitching-moment curve measured at zero lift

[1]See footnote, page 2.

$\frac{dz}{dx}$ slope of the theoretical lifting surface, with respect to a horizontal plane

Subscripts

U upper surface of wing

L lower surface of wing

s superimposed constant-load solution

THEORY

The wing design of the present investigation is the result of a theoretical study of triangular wings performed with two objectives in mind:

(1) The attainment of low drag due to lift at a given design condition. To realize this objective, present knowledge indicates that the wing should have elliptical span load distribution and forward camber.

(2) The development of wing contours with attendant aerodynamic characteristics satisfying item (1), yet yielding large areas which are capable of being generated by straight lines.

The theoretical analysis was based upon linearized lifting-surface theory, for which the principle of superposition of solutions applies. The wing developed by the present investigation was obtained theoretically by the superposition of constant-load sectors of the type derived in reference 8. The slope and ordinate of a sector developed from reference 8 are given as

$$\frac{dz}{dx} = \frac{\beta \frac{\Delta p}{q}}{4\pi m}\left[\sqrt{1-m^2}\left(\cosh^{-1}\frac{x-\beta y m}{|\beta y - mx|} + \cosh^{-1}\frac{x+\beta y m}{|\beta y + mx|}\right) - 2\cosh^{-1}\frac{x}{|\beta y|}\right] \tag{1}$$

$$z = \int_{\xi}^{x} \frac{dz}{dx}\,dx \tag{2}$$

It can be seen from an examination of equation (1) that at the plane of symmetry (y=0) the term $\cosh^{-1}\frac{x}{|\beta y|}$ becomes infinite, resulting in a singularity in the slope and ordinate of the constant-load surface. This singularity may be removed by superimposing an infinite number of solutions, described by equation (1), of such loading ($\Delta p/q$) and apex angle (m) that the summation of terms eliminates the singularity. One relationship between the loading of each superimposed sector $\left(\frac{d\Delta p/q}{dm}\right)$ and the apex angle (m) is

$$\frac{d\left(\frac{\Delta p}{q}\right)}{dm} = -\frac{n(n+2)}{2m_o^{(n+1)}} C_{L_{des}} m^n \qquad (3)$$

The value of n in equation (3) determines the shape of the span load distribution. Figure 1 shows various span load distributions obtainable for several selected values of n. For the present investigation, a value of n=3 was chosen since the resulting span load distribution is nearly elliptical. (See fig. 1.) The following integral relation for n=3 defines the slope of a lifting surface which has no singularity at the plane of symmetry and which supports a nearly elliptical span load distribution:

$$\frac{dz}{dx} = \frac{5\beta C_{L_{des}}}{8\pi}\left[\frac{\sqrt{1-m_o^2}}{m_o}\left(\cosh^{-1}\frac{x-m_o\beta y}{|\beta y-m_o x|} + \cosh^{-1}\frac{x+m_o y\beta}{|\beta y+m_o x|}\right)\right] -$$

$$\frac{15\beta C_{L_{des}}}{8\pi m_o^4}\int_0^{m_o} m^2\sqrt{1-m^2}\left(\cosh^{-1}\frac{x-\beta my}{|\beta y-mx|} + \cosh^{-1}\frac{x+\beta my}{|\beta y+mx|}\right)dm \qquad (4)$$

The trace in a vertical plane perpendicular to the flight direction of the leading edge and trailing edge of the wing plan form of the present investigation designed for a lift coefficient of 0.25 at a Mach number of 1.53 is shown in figure 2(a).

To satisfy the preceding item (2), the theoretical surface was altered. The modification consisted, first, of removing the curvature of the cambered surface over the central 80-percent local semispan region. This modification, for all spanwise sections, is the same as that shown in figure 2(a) for the trailing-edge section. The surface was then altered further by shearing all streamwise sections downward a distance proportional to the spanwise distance from the plane of

symmetry in order to bring all elements of the central portion of both wing panels into one plane. Linearized theory would predict no load change from such a modification. The distance the sections must be sheared is expressed by the following equation:

$$\Delta Z = -0.1466\left(\frac{2y}{b}\right)c_r \qquad (5)$$

For the wing of the present investigation, the design lift coefficient was 0.25 and the design Mach number was 1.53. An NACA 0003-63 airfoil section was used as the thickness distribution in combination with the mean lines of the modified and sheared wing to make up the streamwise airfoil sections. The streamwise section coordinates for this wing are given in table I.

APPARATUS

Wind Tunnel and Equipment

The experimental investigation was conducted in the Ames 6- by 6-foot supersonic wind tunnel. In this wind tunnel, the Mach number can be varied continuously and the stagnation pressure regulated to maintain a given test Reynolds number. The air is dried to prevent formation of condensation shocks. Further information on this wind tunnel is presented in reference 9.

The model was sting-mounted in the wind tunnel, the diameter of the sting being about 73 percent of the diameter of the body base. The pitch plane of the model support was horizontal. The 4-inch-diameter, four-component, strain-gage balance, described in reference 10, was enclosed within the body of the model and was used to measure the aerodynamic forces and moments.

Model

A photograph of the model is shown in figure 3. A plan view of the model and certain model dimensions are given in figure 4. Other important geometric characteristics of the model are as follows:

Wing

Aspect ratio	2
Taper ratio	0
Thickness distribution (streamwise)	NACA 0003-63
Total area, S, square feet	4.014
Mean aerodynamic chord, $\bar{c}$, feet	1.888
Incidence, degrees	0
Distance, wing reference plane to body axis, feet	0

Body

Fineness ratio (based upon length, l, fig. 4)	12.5
Cross-section shape	Circular
Maximum cross-sectional area, square feet	0.204
Ratio of maximum cross-sectional area to wing area	0.0509

The wing was constructed of solid steel. The body spar was also steel and covered with aluminum to form the body contours. The surfaces of the wing and body were polished smooth.

TESTS AND PROCEDURE

Range of Test Variables

The aerodynamic characteristics of the model (as a function of angle of attack) were investigated for a range of Mach numbers from 0.60 to 0.90 and from 1.30 to 1.70 at Reynolds numbers of 3.0 million and 7.5 million.

Reduction of Data

The test data have been reduced to standard NACA coefficient form. Factors which could affect the accuracy of these results, together with the corrections applied, are discussed in the following paragraphs.

Tunnel-wall interference.- Corrections to the subsonic results for the induced effects of the tunnel walls resulting from lift on the model were made according to the methods of reference 11. The numerical values of these corrections (which were added to the uncorrected data) were obtained from

$$\Delta\alpha = 0.93\ C_L$$

$$\Delta C_D = 0.016\ C_L^2$$

No corrections were made to the pitching-moment coefficients.

The effects of constriction of the flow at subsonic speeds by the tunnel walls were taken into account by the method of reference 12. This correction was calculated for conditions at zero angle of attack and was applied throughout the angle-of-attack range. At a Mach number of 0.90, this correction amounted to a 4-percent increase in the Mach number and in the dynamic pressure over that determined from a calibration of the wind tunnel without a model in place.

For the tests at supersonic speeds, the reflection from the tunnel walls of the Mach wave originating at the nose of the body did not cross the model. No corrections were required, therefore, for tunnel-wall effects.

Stream variations.- Tests of the present model at subsonic speeds in both the normal and the inverted positions have indicated a slight stream inclination and curvature in the pitch plane of the model. Results of these tests indicate that a 0.07° stream angle, and a stream curvature capable of producing a pitching-moment coefficient of -0.002, exist throughout the subsonic speed range. The slope parameters $dC_L/d\alpha$ and dC_m/dC_L were unaffected, however. No corrections, for the effect of the stream irregularities, were made to the data of the present investigation. At subsonic speeds the longitudinal variation of static pressure in the region of the model is not known accurately at present, but a preliminary survey has indicated that it is less than 2 percent of the dynamic pressure. No correction for this effect was made.

A survey of the air stream in the wind tunnel at supersonic speeds (reference 9) has shown a stream curvature only in the yaw plane of the model. The effects of this curvature on the measured characteristics of the present model are not known, but are believed to be small as judged by the results of reference 13. The survey of reference 9 also indicated that there is a static-pressure variation in the test section of sufficient magnitude to affect the drag results. A correction was added to the measured drag coefficient, therefore, to account for the longitudinal buoyancy caused by this static-pressure variation. This correction varied from as much as -0.0008 at a Mach number of 1.30 to +0.0009 at a Mach number of 1.70.

Support interference.– At subsonic speeds, the effects of support interference on the aerodynamic characteristics of the model are not known. For the present tailless model, it is believed that such effects consisted primarily of a change in the pressure at the base of the model. In an effort to correct at least partially for this support interference, the base pressure was measured and the drag data were adjusted to correspond to a base pressure equal to the static pressure of the free stream.

At supersonic speeds, the effects of support interference of a body-sting configuration similar to that of the present model are shown by reference 14 to be confined to a change in base pressure. The previously mentioned adjustment of the drag for base pressure, therefore, was applied at supersonic speeds.

RESULTS

The results are presented in this report without analysis in order to expedite publication. The variation of lift coefficient with angle of attack and the variation of pitching-moment coefficient, drag, coefficient, and lift-drag ratio with lift coefficient at Reynolds numbers of 3.0 million and 7.5 million and at Mach numbers from 0.60 to 1.70 are shown in figure 5. The results of figure 5, for a Reynolds number of 7.5 million, have been summarized in figure 6 to show the important parameters as functions of Mach number. The slope parameters in this figure have been measured at zero lift.

Ames Aeronautical Laboratory,
National Advisory Committee for Aeronautics,
Moffett Field, Calif.

REFERENCES

1. Smith, Donald W., and Heitmeyer, John C.: Lift, Drag, and Pitching Moment of Low-Aspect-Ratio Wings at Subsonic and Supersonic Speeds – Plane Triangular Wing of Aspect Ratio 2 With NACA 0008-63 Section. NACA RM A50K20, 1951.

2. Smith, Donald W., and Heitmeyer, John C.: Lift, Drag, and Pitching Moment of Low-Aspect-Ratio Wings at Subsonic and Supersonic Speeds – Plane Triangular Wing of Aspect Ratio 2 With NACA 0005-63 Section. NACA RM A50K21, 1951.

3. Heitmeyer, John C., and Stephenson, Jack D.: Lift, Drag and Pitching Moment of Low-Aspect-Ratio Wings at Subsonic and Supersonic Speeds – Plane Triangular Wing of Aspect Ratio 4 With NACA 0005-63 Section. NACA RM A50K24, 1951.

4. Phelps, E. Ray, and Smith, Willard G.: Lift, Drag, and Pitching Moment of Low-Aspect-Ratio Wings at Subsonic and Supersonic Speeds – Triangular Wing of Aspect Ratio 4 With NACA 0005-63 Thickness Distribution, Cambered and Twisted for Trapezoidal Span Load Distribution. NACA RM A50K24b, 1951.

5. Heitmeyer, John C., and Smith, Willard G.: Lift, Drag, and Pitching Moment of Low-Aspect-Ratio Wings at Subsonic and Supersonic Speeds – Plane Triangular Wing of Aspect Ratio 2 With NACA 0003-63 Section. NACA RM A50K24a, 1951.

6. Smith, Willard G., and Phelps, E. Ray: Lift, Drag, and Pitching Moment of Low-Aspect-Ratio Wings at Subsonic and Supersonic Speeds – Triangular Wing of Aspect Ratio 2 With NACA 0005-63 Thickness Distribution, Cambered and Twisted for Trapezoidal Span Load Distribution. NACA A50K27a, 1951.

7. Reese, David E., and Phelps, E. Ray: Lift, Drag, and Pitching Moment of Low-Aspect-Ratio Wings at Subsonic and Supersonic Speeds – Plane Tapered Wing of Aspect Ratio 3.1 With 3-Percent Thick Biconvex Section. NACA RM A50K28, 1951.

8. Jones, Robert T.: Estimated Lift-Drag Ratios at Supersonic Speeds NACA TN 1350, 1947.

9. Frick, Charles W., and Olson, Robert N.: Flow Studies in the Asymmetric Adjustable Nozzle of the Ames 6- by 6-Foot Supersonic Wind Tunnel. NACA RM A9E24, 1949.

10. Olson, Robert N., and Mead, Merrill H.: Aerodynamic Study of a Wing-Fuselage Combination Employing a Wing Swept Back 63° – Effectiveness of an Elevon as a Longitudinal Control and the Effects of Camber and Twist on the Maximum Lift-Drag Ratio at Supersonic Speeds. NACA RM A50A31a, 1950.

11. Glauert, H.: Wind Tunnel Interference on Wings, Bodies, and Airscrews. R.&M. No. 1566, British, 1933.

12. Herriot, John G.: Blockage Corrections for Three-Dimensional-Flow Closed-Throat Wind Tunnels, with Consideration of the Effect of Compressibility. NACA Rep. 995, 1950. (Formerly NACA RM A7B28)

13. Lessing, Henry C.: Aerodynamic Study of a Wing–Fuselage Combination Employing a Wing Swept Back 63° – Effect of Sideslip on Aerodynamic Characteristics at a Mach Number of 1.4 With the Wing Twisted and Cambered. NACA RM A50F09, 1950.

14. Perkins, Edward W.: Experimental Investigation of the Effects of Support Interference on the Drag of Bodies of Revolution at a Mach Number of 1.5. NACA RM A8B05, 1948.

TABLE I[2].- COORDINATES IN INCHES OF THE APPROXIMATELY ELLIPTICAL SPAN LOAD, TWISTED AND CAMBERED ASPECT RATIO 2 TRIANGULAR WING

Station 0		Station 3.4				Station 6.8			
X	Z	X_U	Z_U	X_L	Z_L	X_U	Z_U	X_L	Z_L
0	0	0	−0.142	0	−0.142	0	−0.284	0	−0.284
.425	.161	.314	.061	.349	−.194	.225	−.111	.268	−.299
.850	.222	.655	.149	.681	−.210	.475	−.028	.518	−.291
1.700	.302	1.340	.239	1.350	−.245	.983	.086	1.019	−.274
2.551	.357	2.025	.285	2.025	−.285	1.493	.159	1.521	−.269
3.401	.398	2.706	.318	2.706	−.318	2.006	.211	2.025	−.266
5.101	.455	4.067	.364	4.067	−.364	3.031	.273	3.037	−.263
6.801	.488	5.428	.390	5.428	−.390	4.055	.293	4.055	−.292
8.502	.505	6.788	.404	6.788	−.404	5.077	.301	5.077	−.305
10.202	.510	8.149	.409	8.149	−.409	6.099	.304	6.099	−.308
11.903	.506	9.510	.405	9.510	−.405	7.121	.301	7.121	−.305
13.603	.493	10.871	.395	10.871	−.395	8.142	.298	8.142	−.301
17.004	.450	13.593	.360	13.593	−.360	10.186	.271	10.186	−.272
20.404	.388	16.314	.310	16.314	−.310	12.229	.232	12.229	−.233
23.805	.312	19.036	.250	19.036	−.250	14.273	.187	14.273	−.187
27.206	.223	21.757	.178	21.757	−.178	16.316	.134	16.316	−.134
30.607	.123	24.479	.099	24.479	−.099	18.359	.072	18.359	−.072
32.307	.069	25.840	.055	25.840	−.055	19.381	.041	19.381	−.041
34.007	.011	27.200	.008	27.200	−.008	20.403	.006	20.403	−.006
L.E. radius = 0.034		L.E. radius = 0.027				L.E. radius = 0.020			

Station 10.2				Station 13.6				Station 15.3			
X_U	Z_U	X_L	Z_L	X_U	Z_U	X_L	Z_L	X_U	Z_U	X_L	Z_L
0	−0.426	0	−0.426	0	−0.568	0	−0.568	0	−0.654	0	−0.654
.145	−.302	.182	−.425	.069	−.508	.054	−.571	.033	−.619	.048	−.648
.308	−.233	.350	−.406	.151	−.463	.178	−.548	.073	−.594	.081	−.638
.642	−.132	.684	−.370	.315	−.398	.346	−.515	.156	−.560	.176	−.618
.978	−.057	1.017	−.340	.481	−.343	.513	−.482	.238	−.529	.258	−.593
1.317	−.001	1.352	−.317	.649	−.298	.681	−.455	.490	−.445	.511	−.534
1.996	.086	2.023	−.277	.986	−.226	1.016	−.406	.659	−.404	.680	−.500
2.678	.140	2.697	−.249	1.326	−.172	1.352	−.363	.829	−.367	.848	−.467
3.360	.174	3.373	−.230	1.665	−.124	1.689	−.325	.998	−.331	1.016	−.433
4.043	.195	4.050	−.214	2.006	−.084	2.026	−.288	1.169	−.306	1.186	−.407
4.726	.202	4.729	−.204	2.346	−.056	2.366	−.258	1.340	−.282	1.355	−.381
5.410	.198	5.410	−.198	2.689	−.032	2.703	−.230	1.683	−.242	1.694	−.332
6.774	.180	6.774	−.180	3.372	.004	3.382	−.178	2.025	−.207	2.034	−.285
8.138	.156	8.138	−.156	4.056	.022	4.063	−.134	2.369	−.180	2.375	−.243
9.503	.125	9.503	−.125	4.742	.031	4.746	−.094	2.712	−.154	2.715	−.199
10.867	.089	10.867	−.089	5.387	.032	5.389	−.057	3.056	−.140	3.058	−.165
12.231	.049	12.231	−.049	6.113	.025	6.113	−.024	3.228	−.134	3.229	−.148
12.914	.027	12.914	−.027	6.456	.015	6.456	−.013	3.400	−.126	3.400	−.124
13.596	.004	13.596	−.004	6.799	.002	6.799	−.002				
L.E. radius = 0.014				L.E. radius = 0.007				L.E. radius = 0.003			
Station 17.0 X = 0 Z = −0.710											

[2]Location of stations are measured in inches from plane of symmetry.

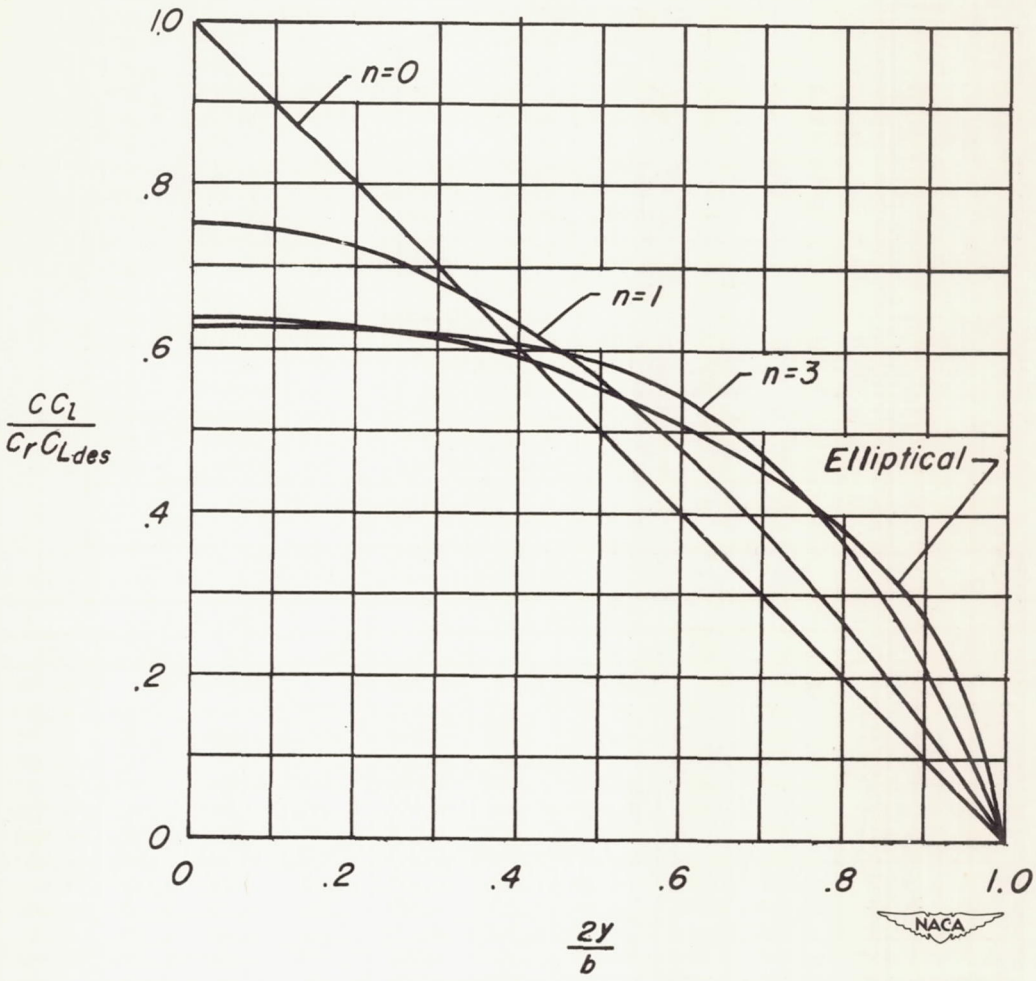

Figure 1.- The span load distributions, corresponding to various values of n, as compared to an elliptical span load distribution.

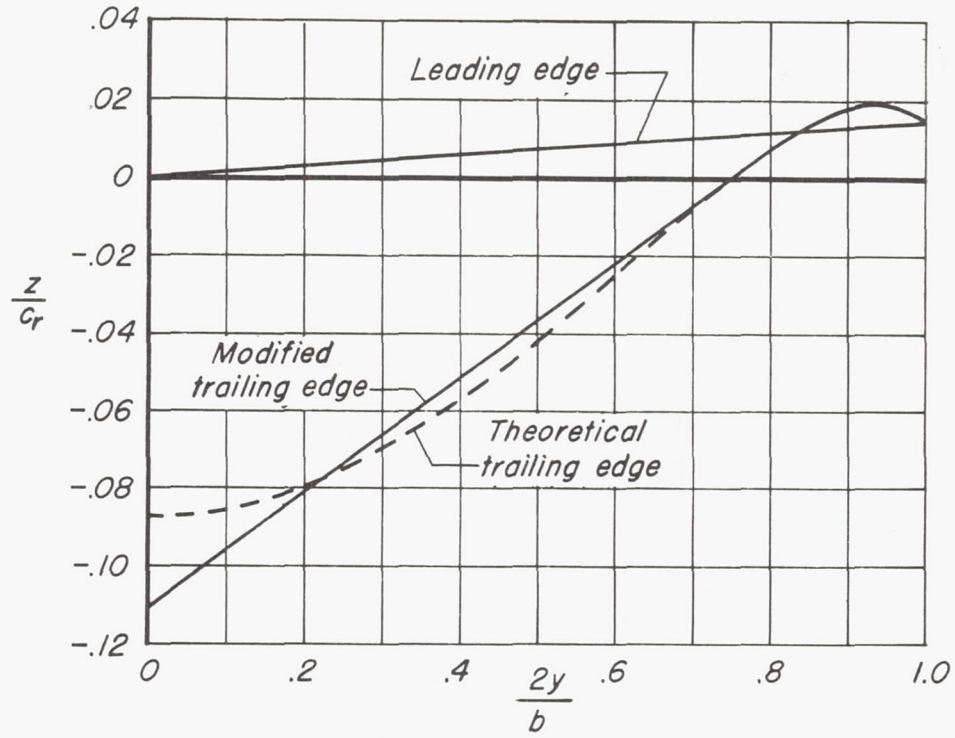

(a) Theoretical wing and modified wing.

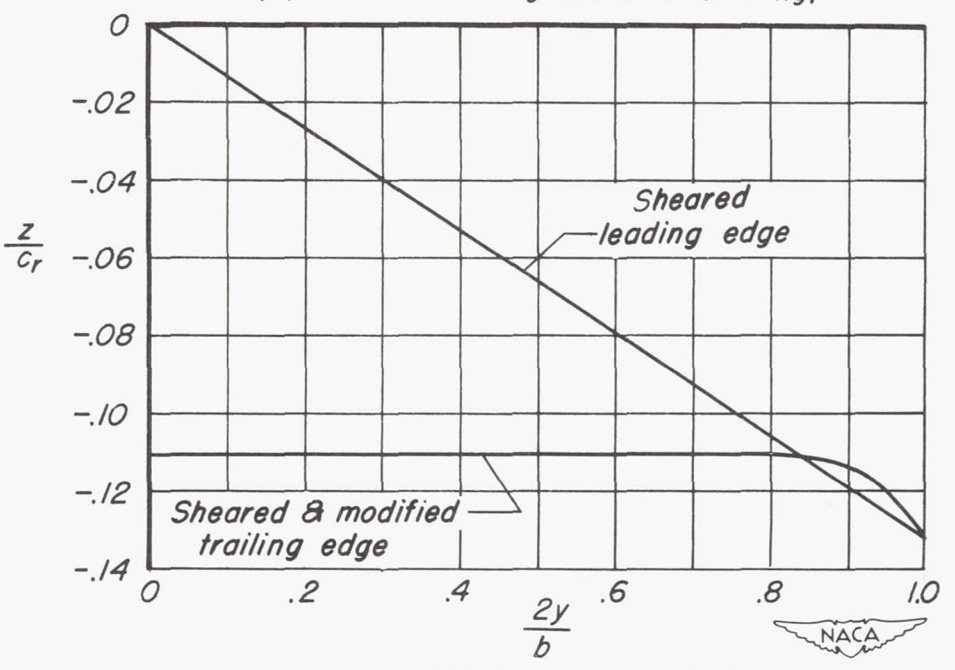

(b) Modified and sheared wing.

Figure 2.-Traces of the leading edge and of the trailing edge for the various wings. m_o, 0.577; $C_{L_{des}}$, 0.25.

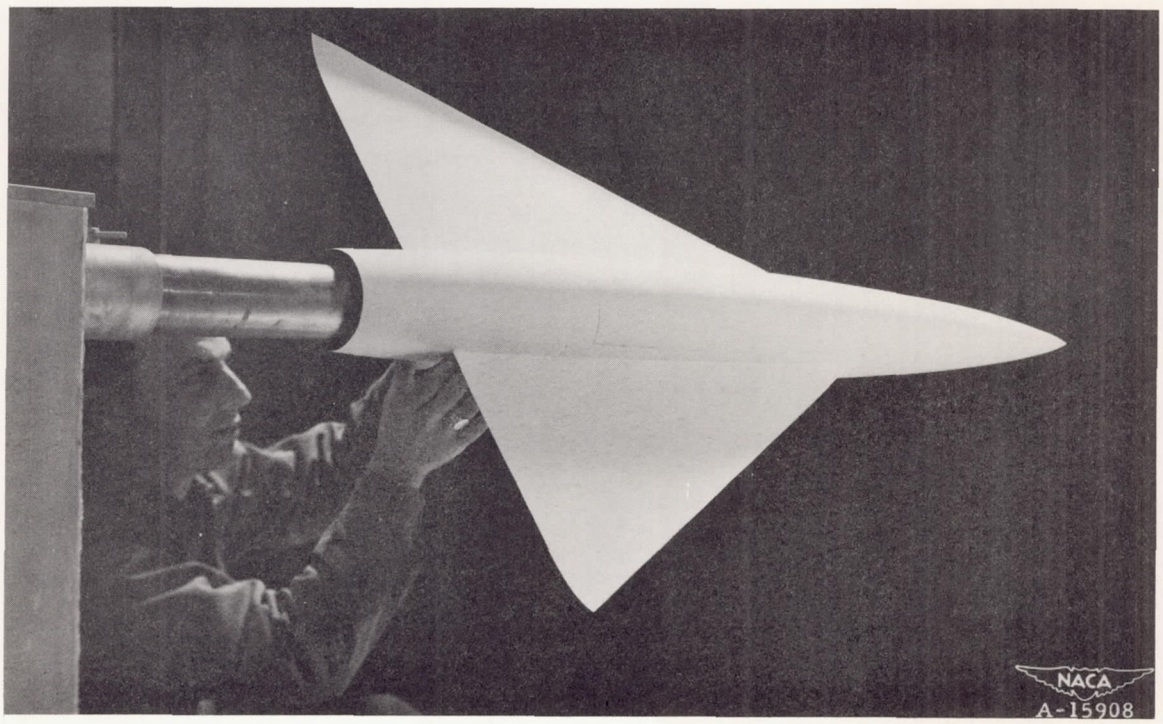

Figure 3.– Photograph of the model in an inverted position.

Equation of fuselage radii:

$$\frac{r}{r_0} = \left[1-\left(1-\frac{2x'}{l}\right)^2\right]^{3/4}$$

All dimensions shown in inches

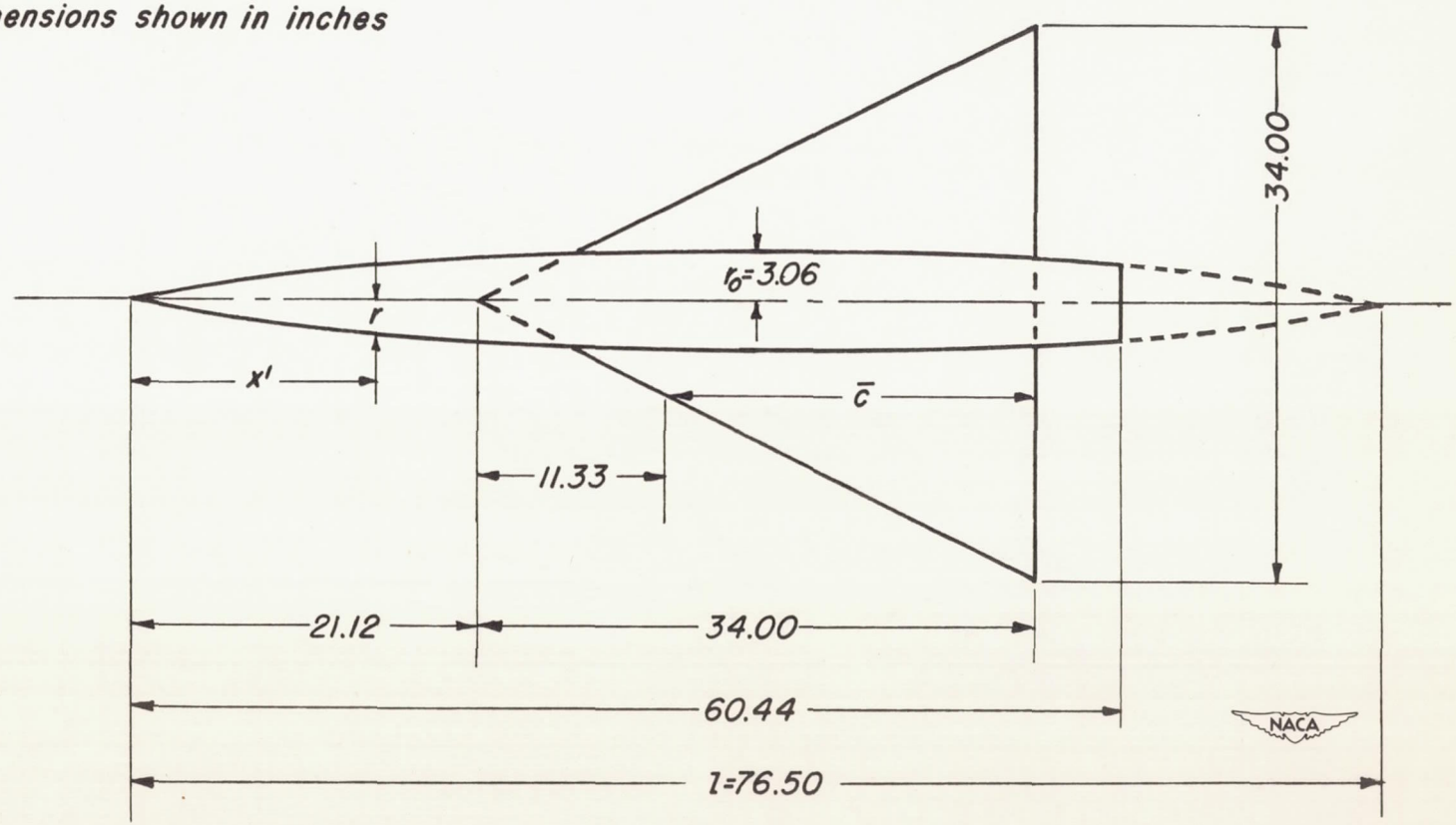

Figure 4.– Plan view of the model.

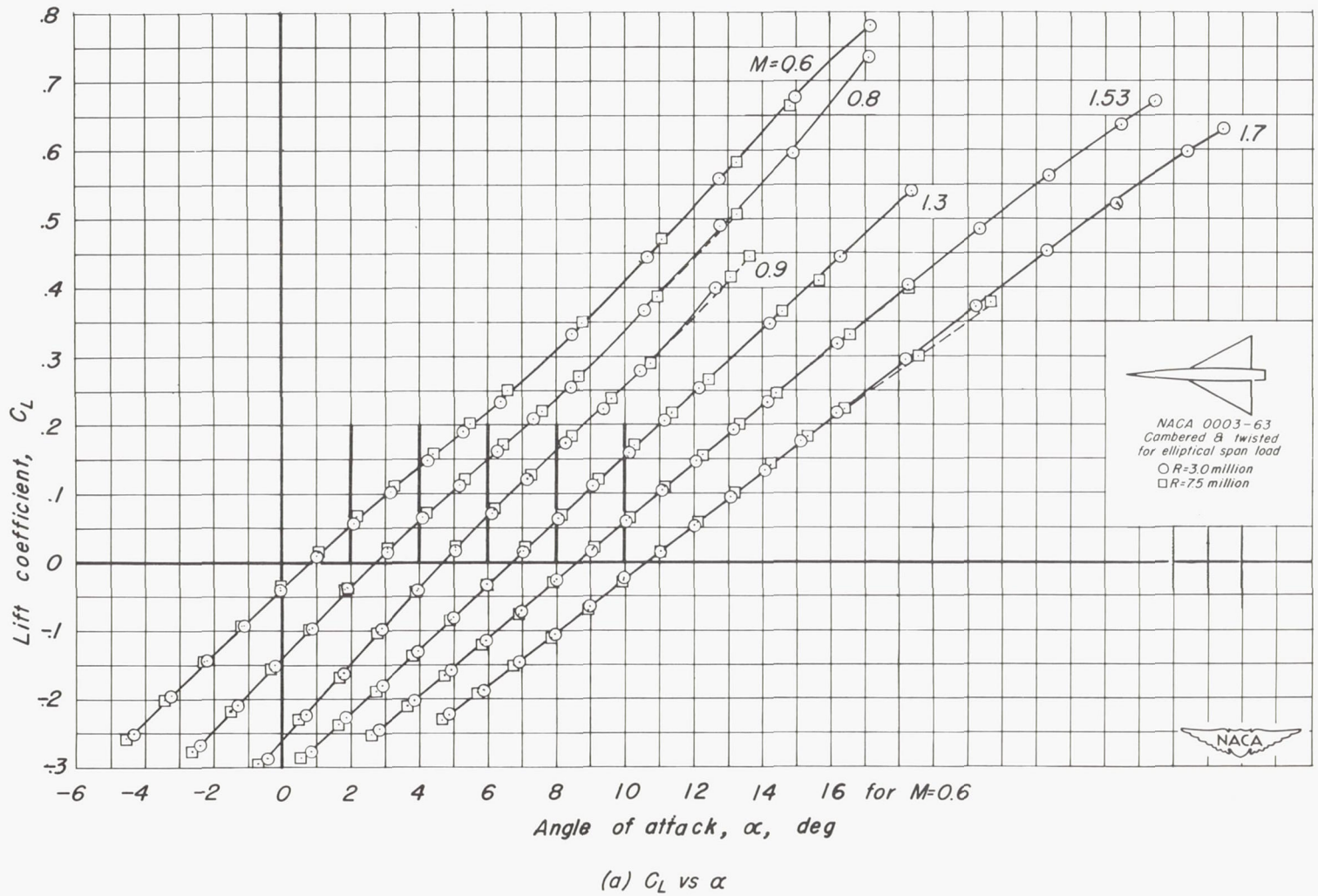

(a) C_L vs α

Figure 5.- The variation of the aerodynamic characteristics with lift coefficient at various Mach numbers.

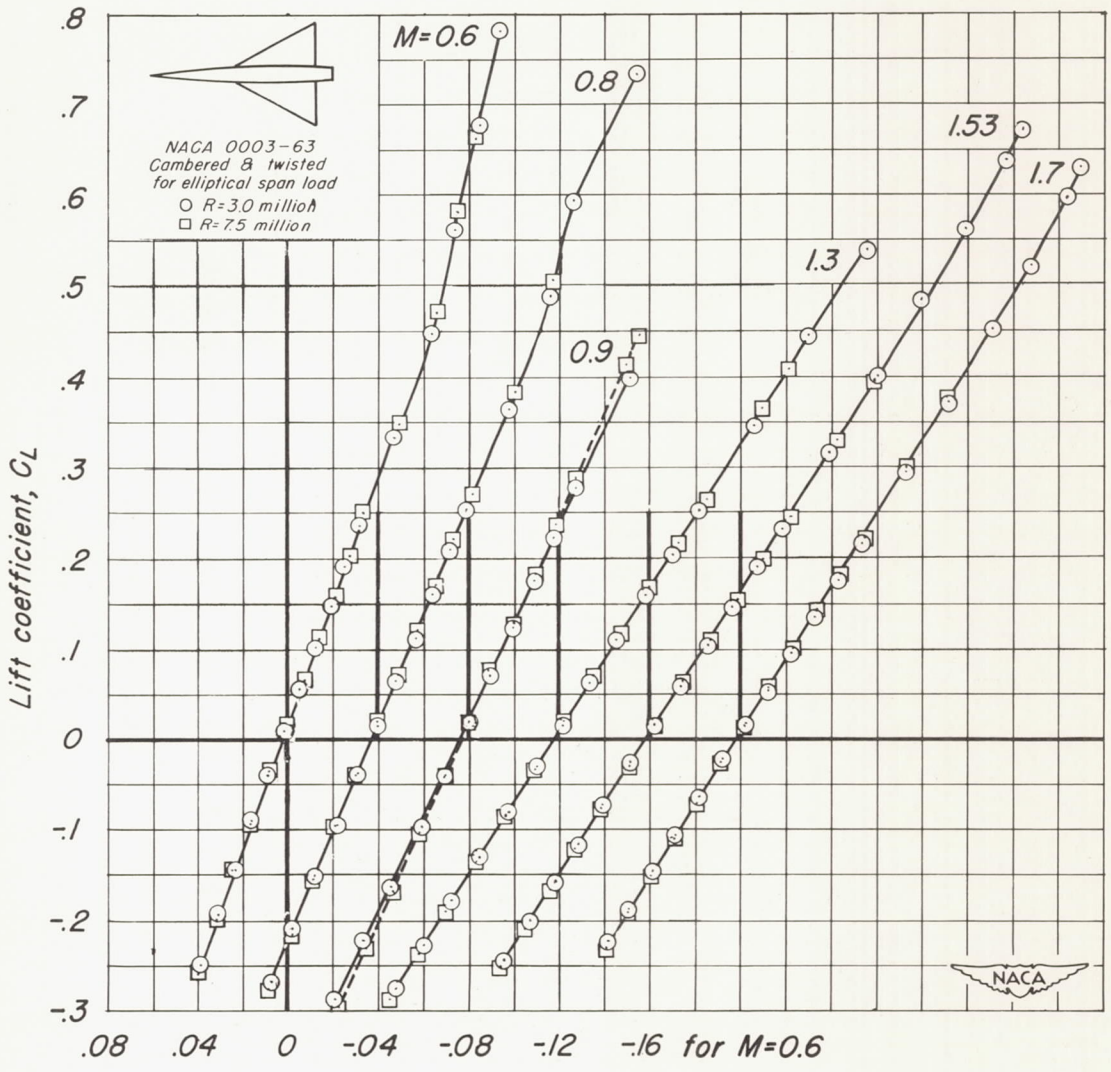

(b) C_L vs C_m

Figure 5.- Continued.

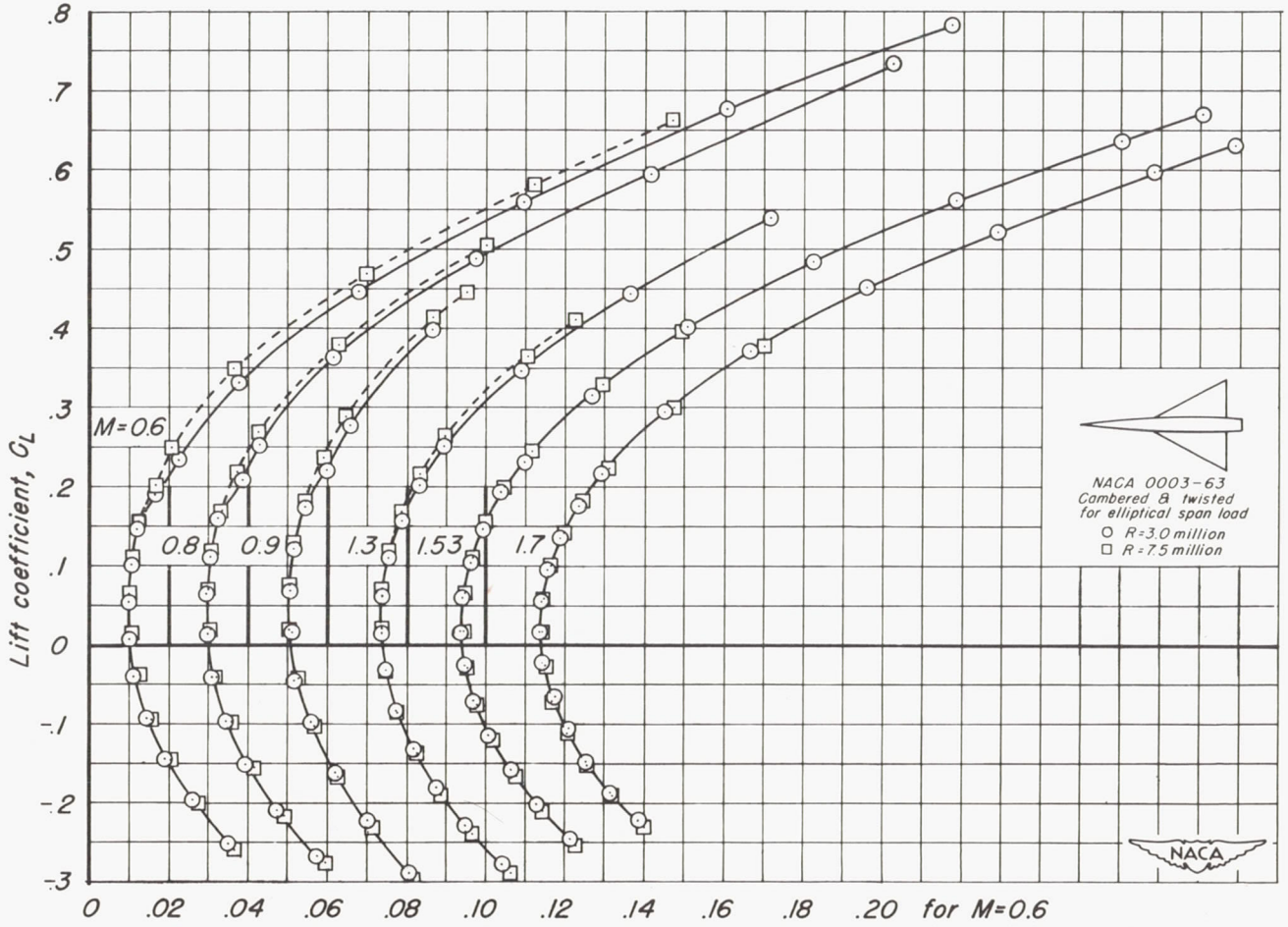

(c) C_L vs C_D

Figure 5.- Continued.

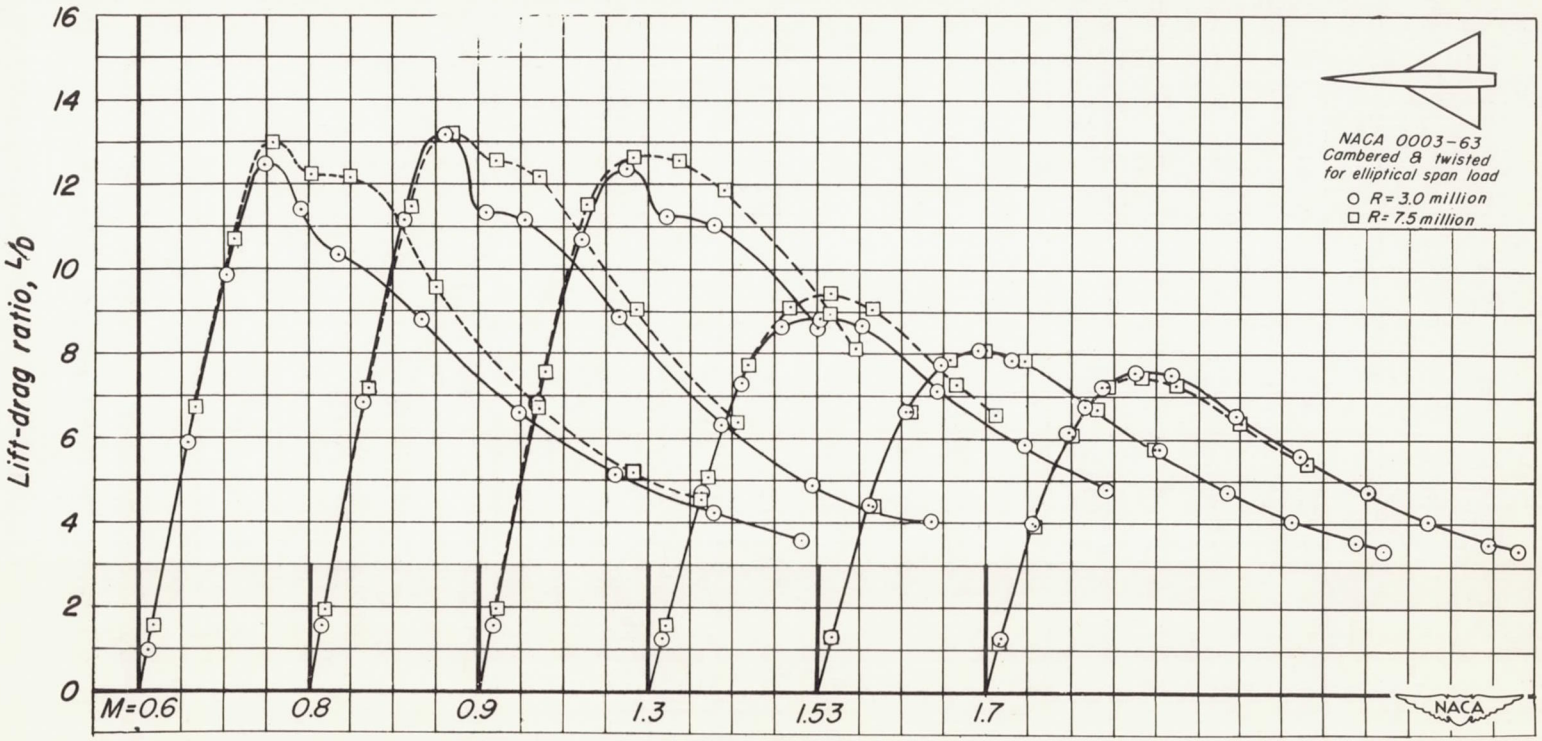

(d) L/D vs C_L

Figure 5.- Concluded.

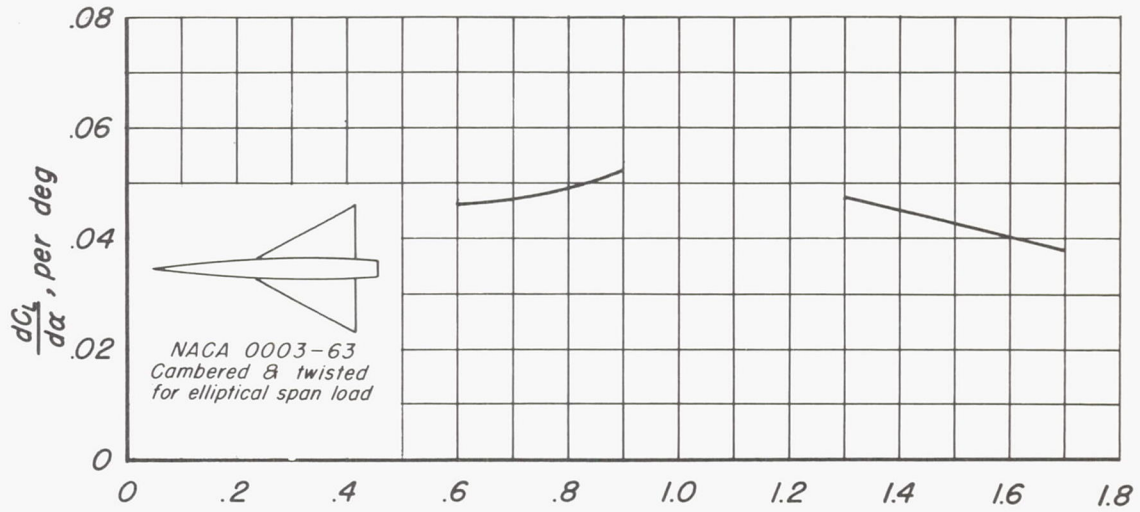

(a) $\frac{dC_L}{d\alpha}$ vs M

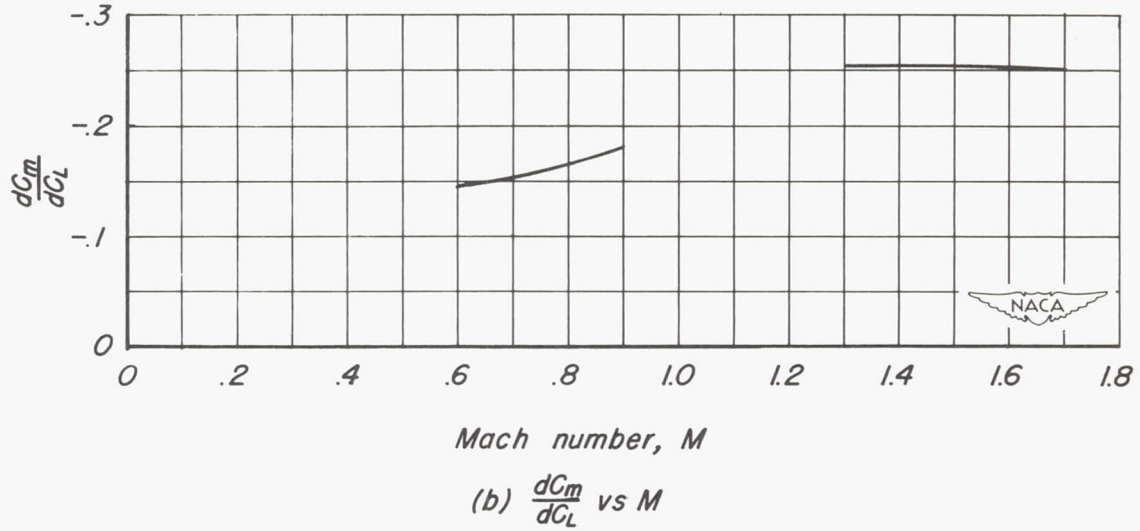

(b) $\frac{dC_m}{dC_L}$ vs M

Figure 6.– Summary of aerodynamic characteristics as a function of Mach number. Reynolds number, 7.5 million.

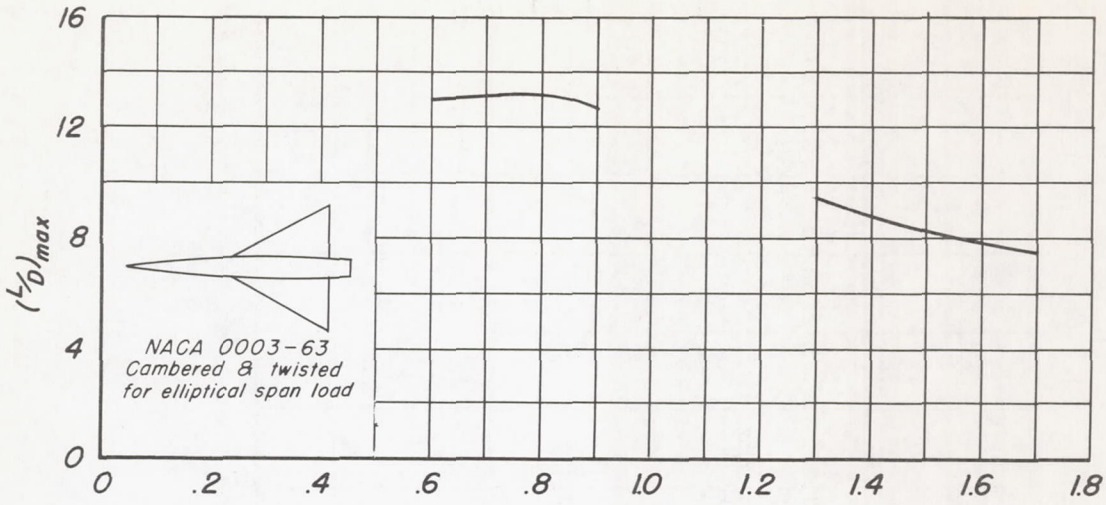

(c) $(L/D)_{max}$ vs M

(d) C_L for $(L/D)_{max}$ vs M

Figure 6.–Continued.

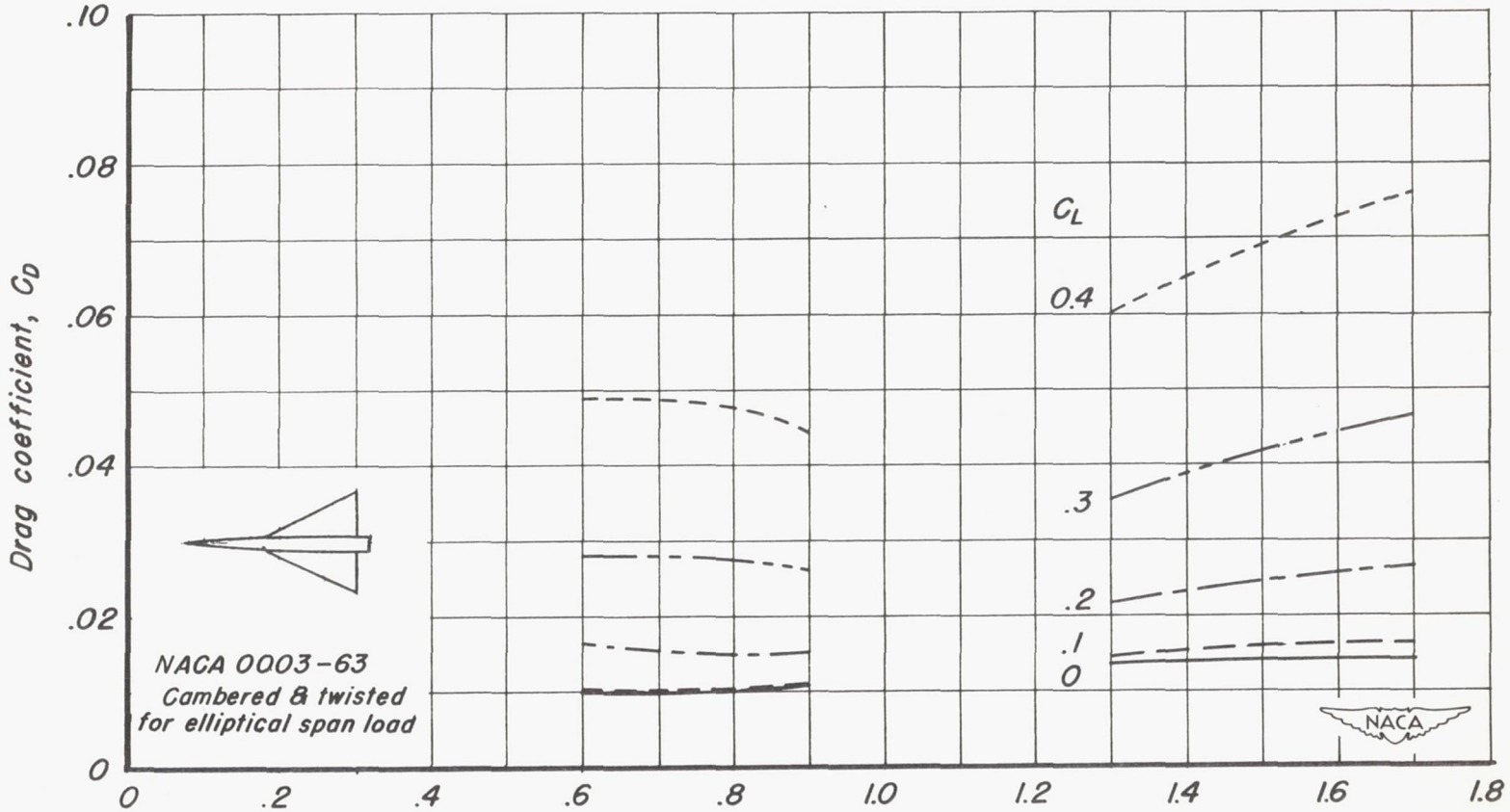

(e) C_D vs M

Figure 6.- Concluded.